New Electrocardiographic Criteria for Discriminating Between Brugada Types 2 and 3 Patterns and Incomplete Right Bundle Branch Block

Stéphane Chevallier, MD,* Andrei Forclaz, MD,* Joanna Tenkorang, MD,* Yannis Ahmad,*
Mohamed Faouzi, MD,† Denis Graf, MD,* Juerg Schlaepfer, MD,* Etienne Pruvot, MD*

Lausanne, Switzerland

Objectives	The aim of this study was to evaluate new electrocardiographic (ECG) criteria for discriminating between incomplete right bundle branch block (RBBB) and the Brugada types 2 and 3 ECG patterns.
Background	Brugada syndrome can manifest as either type 2 or type 3 pattern. The latter should be distinguished from incomplete RBBB, present in 3% of the population.
Methods	Thirty-eight patients with either type 2 or type 3 Brugada pattern that were referred for an antiarrhythmic drug challenge (AAD) were included. Before AAD, 2 angles were measured from ECG leads V_1 and/or V_2 showing incomplete RBBB: 1) α, the angle between a vertical line and the downslope of the r'-wave, and 2) β, the angle between the upslope of the S-wave and the downslope of the r'-wave. Baseline angle values, alone or combined with QRS duration, were compared between patients with negative and positive results on AAD. Receiver-operating characteristic curves were constructed to identify optimal discriminative cutoff values.
Results	The mean β angle was significantly smaller in the 14 patients with negative results on AAD compared to the 24 patients with positive results on AAD ($36 \pm 20°$ vs. $62 \pm 20°$, $p < 0.01$). Its optimal cutoff value was $58°$, which yielded a positive predictive value of 73% and a negative predictive value of 87% for conversion to type 1 pattern on AAD; α was slightly less sensitive and specific compared with β. When the angles were combined with QRS duration, it tended to improve discrimination.
Conclusions	In patients with suspected Brugada syndrome, simple ECG criteria can enable discrimination between incomplete RBBB and types 2 and 3 Brugada patterns. (J Am Coll Cardiol 2011;58:2290–8) © 2011 by the American College of Cardiology Foundation

Three types of Brugada electrocardiographic (ECG) patterns have been described so far (1,2). Although type 1 (coved type) is the hallmark of patients with Brugada syndrome (BrS), types 2 and 3 patterns require antiarrhythmic drug challenge (AAD) to be unmasked and converted into type 1 (3). Types 2 and 3 Brugada patterns are defined as incomplete right bundle branch block (RBBB) with ≥0.1-mV and <0.1-mV ST-segment elevation, respectively, with either a biphasic or a positive T-wave. At present, no descriptive ECG features can differentiate types 2 and 3 Brugada patterns from incomplete RBBB, which is observed in approximately 3% of the population (4,5). We

conducted a prospective study to evaluate newly developed ECG parameters and their ability to predict the AAD response in a population with incomplete RBBB referred to our institution with suspicion of BrS.

Methods

Study population. We included 38 consecutive patients referred to our institution between January 2004 and September 2008 for the evaluation of types 2 and/or 3 Brugada ECG patterns (2). The study was approved by the ethics committee of the University Hospital of Lausanne, and all patients provided oral informed consent. Transthoracic echocardiography and/or magnetic resonance imaging was performed in all patients. Table 1 reports the details of the study population, whose mean age was 40 ± 13 years. Individuals were referred for abnormal ECG findings

(42%), unexplained syncope (42%), and arrhythmia or palpitations (13%).

AAD. All patients underwent AAD consisting of an ajmaline infusion (1 mg/kg body weight, 10 mg/min). The results of the AAD were interpreted by a senior cardiologist (E.P.) specializing in electrophysiology and defined as positive if a type 1 ECG Brugada pattern appeared (2,3).

ECG analysis. The electrodes of the standard 12-lead system were placed according to international recommendations, with leads V_1 and V_2 into the fourth intercostal space (6). The pre-AAD baseline 12-lead electrocardiogram was digitally recorded (filter settings 0.08 to 40 Hz). The analysis included averaging over 3 consecutive beats. The PR and QRS intervals were derived from the longest ECG values. QT intervals were measured in lead V_2. The corrected QT interval was computed using Bazett's formula (corrected $QT = QT/\sqrt{RR}$). Printed versions of the baseline 12-lead electrocardiograms (10 mm/mV and 25 mm/s) were scanned and magnified by a factor of 10. Two angles were measured manually: α, the angle between a vertical line and the downslope of the r'-wave, and β, the angle between the upslope of the S-wave and the downslope of the r'-wave (Fig. 1A).

Reproducibility. Electrocardiograms were analyzed by 2 investigators (S.C. and A.F.) blinded to the results of the AAD. The intraobserver and interobserver reproducibility of angle measurements was assessed on a subset of 32 anonymized electrocardiograms duplicated twice with negative and positive results on AAD (i.e., a total of 3 analyses per patient). The reproducibility of the analysis was assessed for each observer (i.e., intraobserver variability) and between the 2 observers (i.e., interobserver variability).

Simulation of types 2 and 3 Brugada ECG patterns. The underlying pathophysiological mechanisms responsible for BrS ECG patterns remain unknown (7–10). ECGSIM version 2.1.0, an interactive, downloadable Web program (http://www.ecgsim.org), was used to test the 2 main hypotheses debated in the published research, which suggest that disorders of repolarization or of depolarization are the underlying cause of BrS (11–13). ECGSIM computes 12-lead electrocardiograms on the basis of a realistic 3-dimensional representation of epicardial and endocardial action potentials (APs), their local depolarization and repolarization times, and amplitude and diastolic potentials (14). Alterations of the default parameter settings were applied to the center of a circular region (4-cm diameter) covering the epicardial layer of the right ventricular (RV) free wall and right ventricular outflow tract (RVOT) facing lead V_2 (Fig. 2A). The alterations were applied to the center of the circular region shading off until the border (Fig. 2A, external white circle) that interfaced with the unaltered RV epicardial layer.

Statistical analysis. Data analysis was performed using Stata version 11.2 (StataCorp LP, College Station, Texas). The basic statistics listed in Tables 1 and 2 are expressed as mean ± SD. Interobserver reproducibility was assessed using Lin's concordance correlation coefficient, which combines measures of both precision and accuracy to determine how far the observed data deviate from the line of perfect concordance. Intraobserver reproducibility was assessed by computing the intraclass correlation coefficient, with a value of 1 corresponding to a perfect match. The associations of angles and QRS duration with positive results on AAD were assessed using a logistic regression analysis. The strengths of the association were measured by the corresponding odds ratio and p value. Angles and QRS duration were optimally combined in a multivariate predictive model of response to AAD. Receiver-operating characteristic (ROC) curves were constructed, and angles and score cutoff values were chosen to privilege specificity while maintaining high sensitivity. ROC curves were compared using the Delong et al. (15) method.

Results

Cardiac imaging techniques revealed underlying structural heart disease (SHD) in 3 (8%) patients: 1 with biventricular noncompaction, 1 with corrected aortic valvular regurgitation, and 1 with hypertension and concentric left ventricular hypertrophy (Table 1).

AAD. Fourteen of the 38 patients (37%) converted to type 1 Brugada patterns during AAD. Figure 1B shows representative examples of electrocardiograms recorded from lead V_2 in patients with negative (top) and positive (bottom) results on AAD at baseline (left) and at the end of ajmaline infusion (right). Note the coved-type pattern characterized

Abbreviations and Acronyms

AAD = antiarrhythmic drug challenge

AP = action potential

BrS = Brugada syndrome

ECG = electrocardiographic

NPV = negative predictive value

PPV = positive predictive value

RBBB = right bundle branch block

ROC = receiver-operating characteristic curve

RV = right ventricular

RVOT = right ventricular outflow tract

SHD = structural heart disease

Table 1	Clinical Characteristics of the Study Population (n = 38)
Men	33 (87%)
Age (yrs)	40 ± 13
SHD	3 (8%)
Biventricular noncompaction	1 (3%)
Aortic regurgitation	1 (3%)
LVH	1 (3%)
Indication for referral	
Abnormal ECG findings	16 (42%)
Syncope	16 (42%)
Family history of sudden death	4 (11%)
Arrhythmia/palpitations	5 (13%)
Chest pain	2 (5%)

Values are n (%) or mean ± SD.
ECG = electrocardiographic; LVH = concentric left ventricular hypertrophy; SHD = structural heart disease.
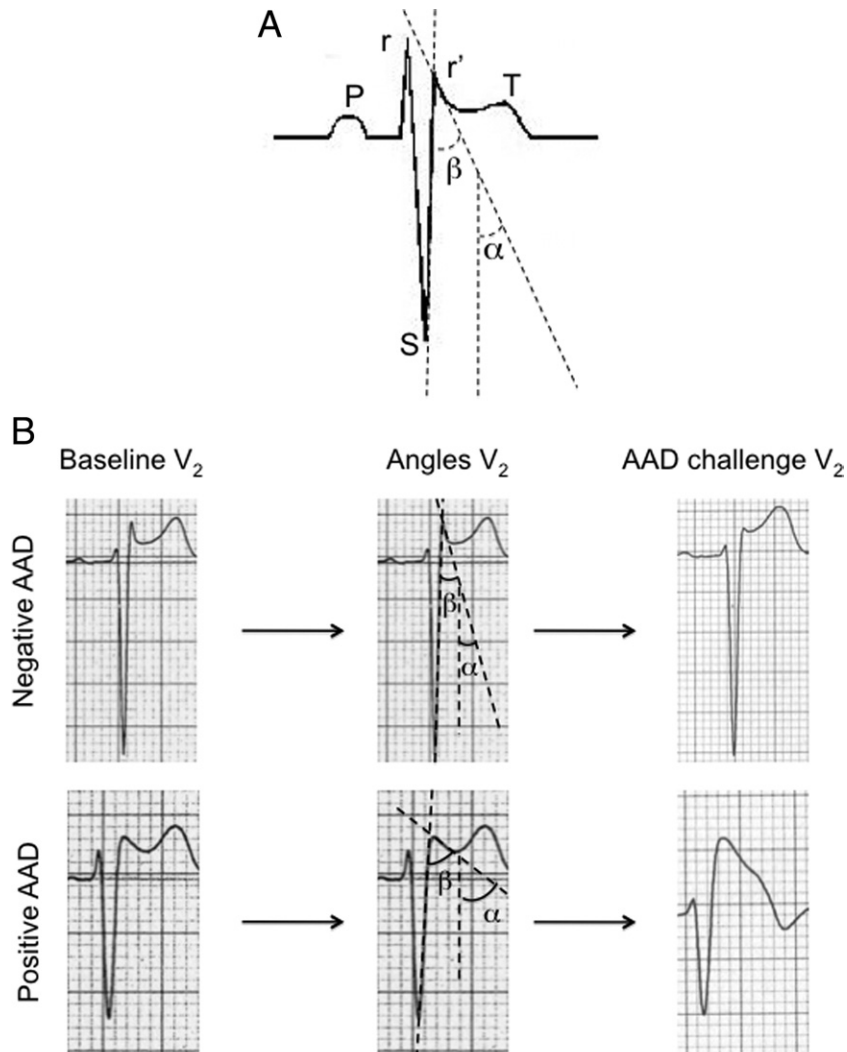
Figure 1 α and β Angle Measurements

(A) Measurements of α and β angles in chest lead V$_2$ displaying an incomplete right bundle branch block (RBBB) pattern; α and β measured 19° and 28°, respectively.
(B) Representative examples of negative **(top row)** and positive **(bottom row)** responses to antiarrhythmic drug challenge (AAD). The **first column** shows lead V$_2$ at baseline. Note that both patients displayed incomplete RBBB pattern with ST-segment elevation typical of type 2 Brugada pattern. The **second column** shows α and β angle measurements, and the **third column** shows lead V$_2$ after ajmaline infusion. The patient with a negative response to AAD had smaller α and β angles compared with the patient with a positive response to AAD (11° and 15° vs. 59° and 66°, respectively).

by atypical RBBB with an inverted T-wave in lead V$_2$ in the patient with positive results on AAD. Table 2 compares the clinical and baseline ECG characteristics of patients with positive and negative results on AAD. Age and the PR and corrected QT intervals were similar between the groups. QRS intervals, however, were significantly prolonged in patients with positive results on AAD (107 ± 21 ms) compared with patients with negative results on AAD (94 ± 9 ms). SHD was present in 1 patient with negative results on AAD and 2 with positive results on AAD.

Angle measurements. Figure 1B shows representative examples of the α and β angles as measured from baseline electrocardiograms. Because β includes the upslope of the

S-wave, its value always exceeds the corresponding α angle value. Although both examples satisfy the definition of type 2 Brugada pattern consisting of an incomplete RBBB pattern with ≥0.1-mV ST-segment elevation in the anterior chest leads, only the patient converting to a type 1 ECG pattern after AAD showed large α and β angles, because of a shallower downslope of the r′-wave. Table 2 also documents baseline ECG mean α and β angle values of patients with negative and positive results on AAD. Both angles were significantly higher in patients who converted to type 1 ECG pattern, but the difference between the groups was found to be greater for β (26°) than α (20°).
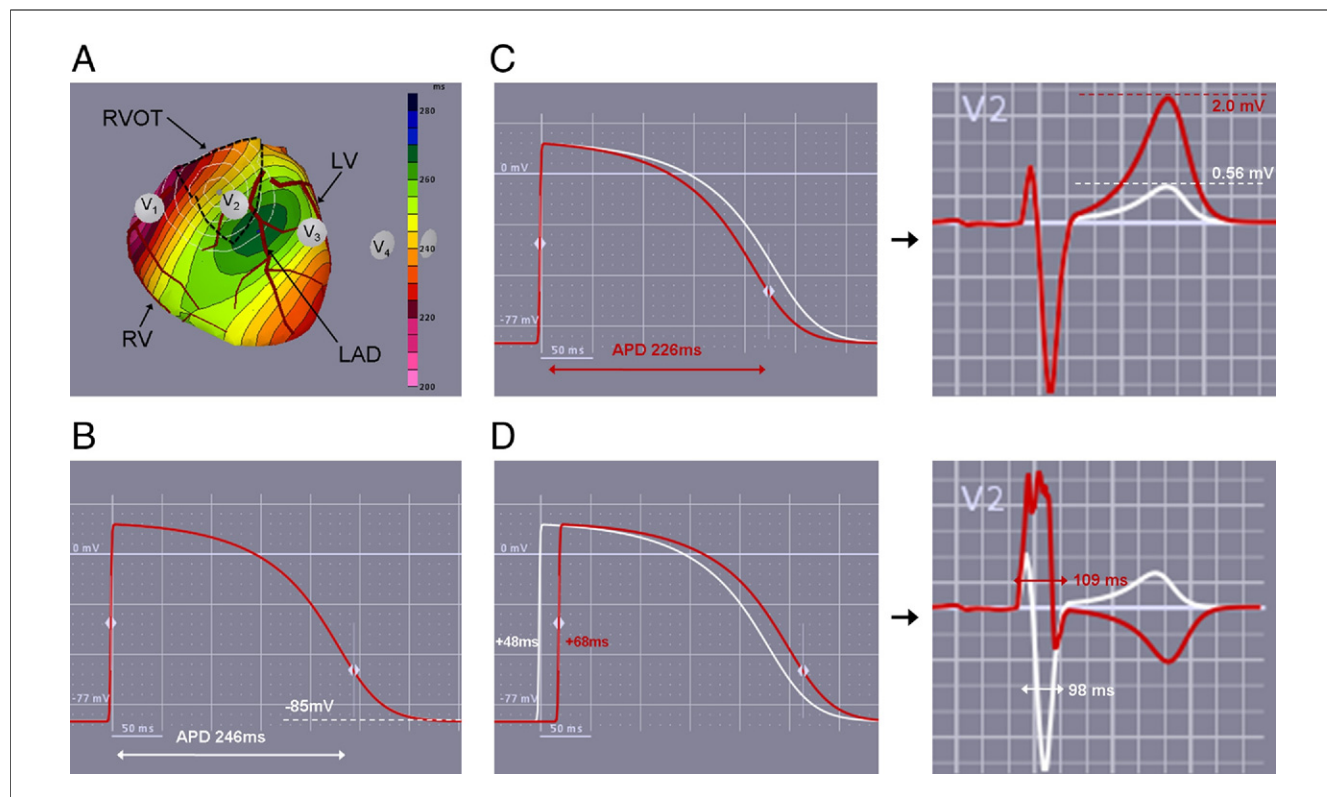
Figure 2 Simulation of Repolarization and Depolarization Hypotheses With ECGSIM

(A) Activation map at baseline (isochrones of 5 ms) of the right ventricle (RV) and left ventricle (LV) separated by the left anterior descending coronary artery (LAD). The right ventricular outflow tract (RVOT) is contoured by a **black dashed line**. The 4-cm epicardial region facing lead V_2 is highlighted by **white circles**. (B) Action potential (AP) of the center of the selected epicardial region shown in A. (C) Decreasing the APs of the selected region (center AP, from 246 to 226 ms) did not produce an ST-segment elevation in lead V_2 (baseline tracing in **white**, altered tracing in **red**) but produced a T-wave of increased amplitude. (D) Delaying APs of the selected region (center AP, from 48 to 68 ms) produced an RBBB pattern with a negative T-wave in lead V_2 but no ST-segment elevation. Abbreviations as in Figure 1.

Figure 3A shows the distribution of baseline α and β angles in patients with negative and positive results on AAD. The overlap between negative and positive results on AAD was smaller for β than for α. Interestingly, some of the outliers (arrows) were patients with SHD (n = 3). Two patients (open arrows), 1 with biventricular noncompaction and the other with corrected aortic valvular disease, displayed narrow α and β angles but positive results on AAD. A third outlier (black arrow) with concentric left ventricular hypertrophy displayed large α and β angles but negative results on AAD.

ROC curves were constructed to identify α and β angle cutoff values that best discriminated between negative and positive results on AAD (Fig. 4). The area under the curve for β (0.8423) (Fig. 4C) was higher than that for α (0.7693) (Fig. 4A). An α cutoff value of >50° yielded sensitivity of 71%, specificity of 79%, a positive predictive value (PPV) of 67%, and a negative predictive value (NPV) of 83% for converting to a type 1 Brugada pattern after AAD. For β, a cutoff value of >58° yielded sensitivity of 79%, specificity of 83%, a PPV of 73%, and an NPV of 87%. The exclusion of patients with SHD increased the sensitivity of α to 83%, the specificity to 83%, the PPV to 71%, and the NPV to 90%, while for β,

the sensitivity increased to 92%, the specificity to 87%, the PPV to 79%, and the NPV to 95%. The interobserver reproducibility for both α and β was 0.99 in lead V_1, while in lead V_2, it was 0.98 and 0.99, respectively. The intraobserver reproducibility was 0.98 (95% confidence interval: 0.97 to 0.99) for S.C. and 0.97 (95% confidence interval: 0.95 to 0.99) for A.F., demonstrating that α and β angles are reproducible measurements that can be performed with confidence by different investigators.

Construction of predictive scores. The angles and QRS duration were combined in a predictive model of response to AAD as follows: 1) α score = 0.068 × α (degrees) + 0.096 × QRS duration (ms); and 2) β score = 0.065 × β (degrees) + 0.081 × QRS duration (ms). Table 2 and Figure 3B report the mean values and distribution of α and β scores in patients with positive and negative results on AAD. An increase in angle value and in QRS duration raised the risk for converting to a type 1 ECG pattern on AAD by 7% and by 9% to 10%, respectively, for each additional degree and millisecond. SHD appeared to affect the distribution of scores less than that of the angles. Figures 4B and 4D show ROC curves, from which score cutoff values were derived that privileged specificity while maintaining high sensitivity. An α score >13.16 classified

Table 2	Baseline Electrocardiographic Indexes of Patients With Negative and Positive Responses to AAD			
Variable	**Negative Results on AAD (n = 24)**	**Positive Results on AAD (n = 14)**	**OR**	**p Value**
Univariate analysis				
Age (yrs)	38 ± 11	44 ± 16	1.04	0.16
Men	22 (92%)	11 (79%)	1.14	0.86
SHD	1 (4%)	2 (14%)	3.83	0.29
PR interval (ms)	154 ± 22	162 ± 27	1.02	0.20
QRS duration (ms)	94 ± 9	107 ± 21	1.08	<0.05
QTc interval (ms)	398 ± 29	413 ± 40	1.02	0.16
α angle (°)	31 ± 19	51 ± 19	1.06	<0.05
β angle (°)	36 ± 20	62 ± 20	1.07	<0.05
Multivariate analysis: α angle				
α angle			1.07	<0.05
QRS duration			1.10	<0.05
Multivariate analysis: β angle				
β angle			1.07	<0.05
QRS duration			1.09	0.06
α score	11.10 ± 1.32	13.78 ± 2.13		<0.05
β score	10.11 ± 1.28	12.89 ± 2.29		<0.05

Values are mean ± SD or n (%).

AAD = antiarrhythmic drug challenge; OR = odds ratio; QTc = corrected QT; SHD = structural heart disease.

patients as positive responders and a score ≤13.16 classified patients as negative responders to AAD, with sensitivity of 79%, specificity of 96%, a PPV of 92%, and an NPV of 88%. Similarly, a β score >11.93 classified patients as positive responders and a score ≤11.93 classified patients as negative responders to AAD, with sensitivity of 79%, specificity of 92%, a PPV of 85%, and an NPV of 88%. Areas under the curves were compared between α and β angles (p = 0.12), α angle and α score (p = 0.23), β angle and β score (p = 0.66), and α score and β score (p = 0.76). No significant differences were observed.

Simulation of ST-segment elevation in Brugada ECG patterns. Figure 2B shows a representative epicardial AP from the center of the selected region before any alteration was applied (AP duration 246 ms, diastolic potential −85 mV). To simulate the repolarization hypothesis, epicardial APs of the selected region (244 ± 14 ms) were shortened in 10-ms steps until the minimal achievable value (139 ± 49 ms) authorized by the program. Figure 2C shows a representative example in which the shortening of epicardial APs (center AP, from 246 to 226 ms) did not produce an ST-segment elevation or an RBBB pattern but did produce a positive T-wave of increased amplitude that was restricted to leads V_1 to V_3 (from 0.56 mV at baseline to 2.0 mV in lead V_2). To test the depolarization hypothesis, the activation time of the selected epicardial region was progressively delayed in 10-ms steps (center AP, from 48 ms at baseline to 148 ms). Figure 2D shows a representative example in which delaying the activation time of the center AP by 20 ms (from 48 to 68 ms) produced an RBBB pattern with a prolonged QRS duration (from 98

ms at baseline to 109 ms in lead V_2) and a negative T-wave (restricted to leads V_1 and V_2) but did not produce an ST-segment elevation.

Discussion

In this study, we sought to evaluate the ability of new ECG indexes to predict the outcomes of AAD in patients fulfilling criteria for type 2 or 3 Brugada pattern. Two different angles, alone and in combination with QRS duration, were measured before ajmaline infusion from anterior chest leads displaying an incomplete RBBB pattern. Patients displaying a type 1 ECG pattern after AAD showed significantly higher angles and scores at baseline than patients with negative results on AAD. These findings suggest that incomplete RBBB can be differentiated from type 2 or 3 Brugada pattern using ECG indexes.

Discriminating types 2 and 3 Brugada patterns and incomplete RBBB. The incomplete RBBB pattern reported in our study population is observed in about 3% of the population (4,5). This pattern is considered a variant of the normal ECG pattern. As the final depolarization of the
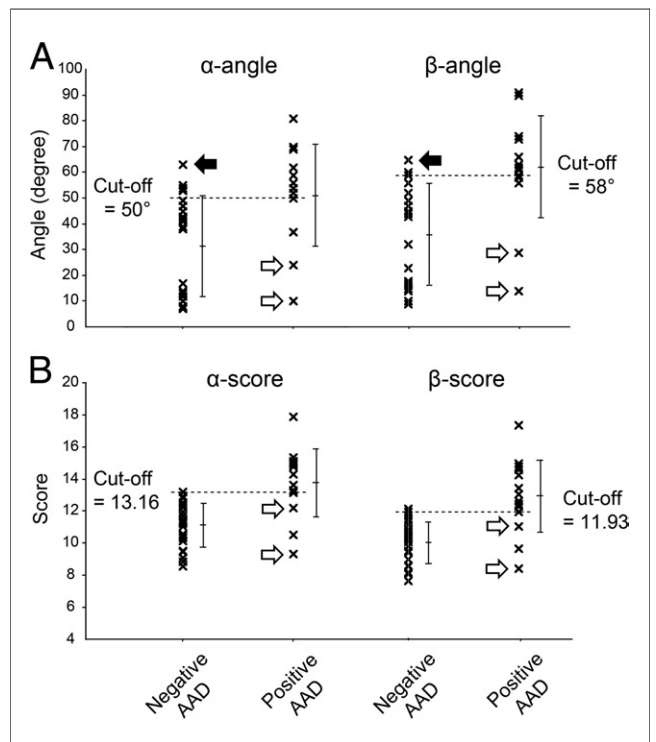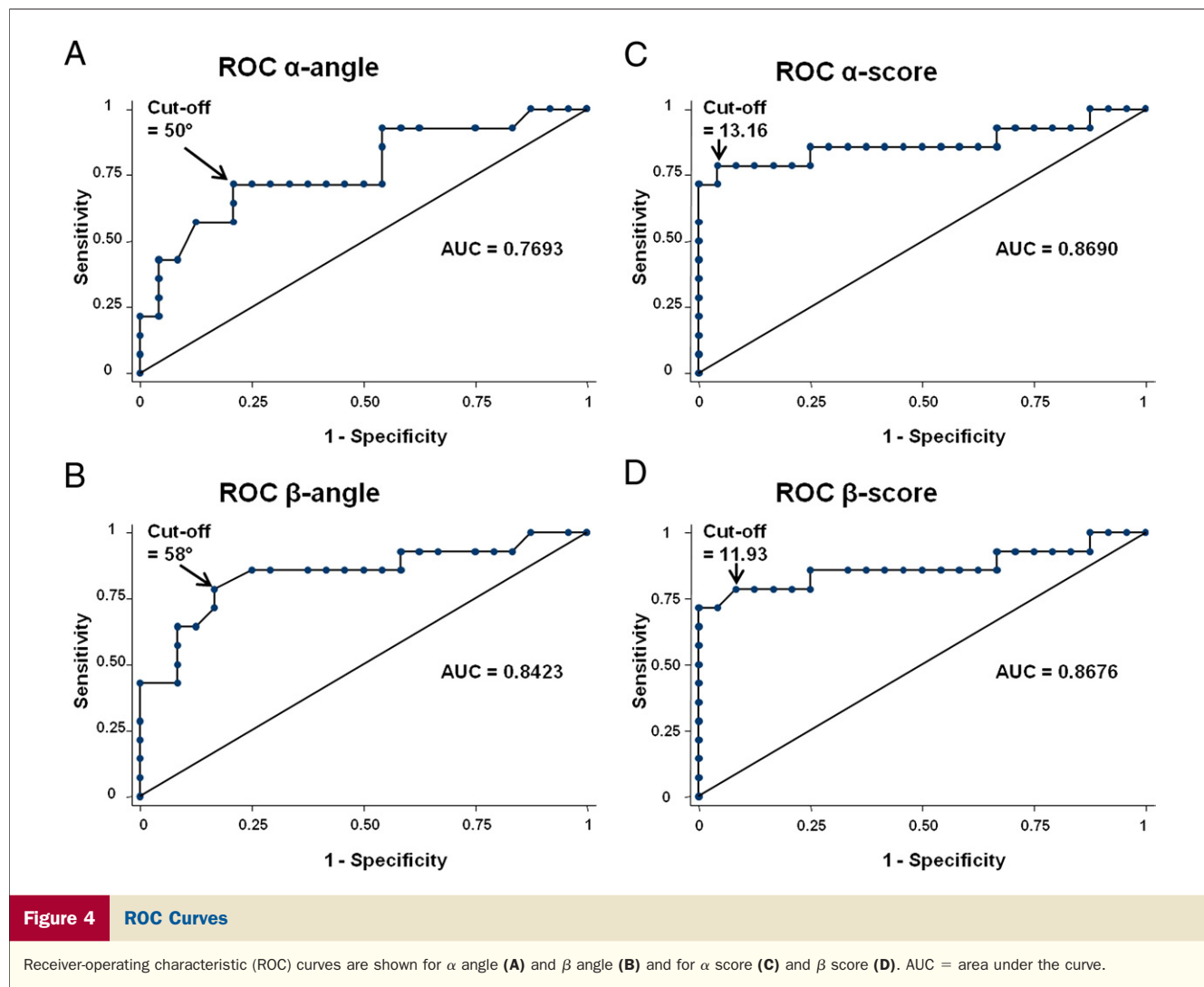

Figure 3	Distribution of Electrocardiographic Angle and Score Values

Distribution of **(A)** α and β angles and **(B)** α and β scores in patients with negative **(first and third columns)** and positive **(second and fourth columns)** responses to antiarrhythmic drug challenge (AAD). Mean and standard deviation are depicted as **vertical lines**. **Plain arrows** indicate the outlier with structural heart disease (SHD) with large angles and a negative response to AAD and open arrows the 2 outliers with SHD with narrow angles, small scores, and positive responses to AAD. **Dashed lines** indicate optimal cut-off values that best discriminated between patients with positive and negative responses to AAD.

Figure 4   ROC Curves

Receiver-operating characteristic (ROC) curves are shown for α angle **(A)** and β angle **(B)** and for α score **(C)** and β score **(D)**. AUC = area under the curve.

right ventricle ends up at the outflow tract and at the heart base (16,17), terminal voltage differences may be directed toward leads V_1 and V_2 and can manifest as an r′-wave. Several studies have attempted to differentiate types 2 and 3 Brugada patterns from incomplete RBBB. Nakazawa et al. (18) subtracted the duration measured from the QRS onset to the peak of the r′-wave in lead V_2 from the duration measured from the QRS onset in lead V_2 to the QRS offset in lead V_5. For a difference ≥0, the NPV of converting to a type 1 Brugada pattern after AAD was 76%. Hermida et al. (19) measured the elevation of the J point in leads V_1 and V_2 placed at the second intercostal space. A J-point elevation ≥ 0.16 mV was specific and highly predictive of the response to AAD, but its sensitivity and NPV were low. We compared 2 angles measured from anterior chest leads, alone and in combination with QRS duration. All indexes reasonably predicted the results of AAD. The area under the curve, NPV, and PPV for angle scores were slightly higher than those for angle values. Interestingly, the exclusion of patients with documented SHD increased the NPV of angle cutoff values to ≥90%. Some SHD can manifest as

Brugada ECG patterns, such as ventricular noncompaction, local inflammation after esophageal surgery, acute ischemia, coronary vasospasm, and coronary anomalies (2,20–22). In our study, the 2 outliers with the smallest α and β angles and positive results on AAD and the patient with the largest angles and negative results on AAD all had SHD. Angle scores appeared less sensitive to SHD than angle values (Fig. 3). These findings confirm the potential confounding effect of SHD on the ability of ECG indexes to predict the response to AAD (2). Intraobserver and interobserver reproducibility was high, suggesting that angle measurements can be used by different adequately trained investigators.

Potential mechanisms of ST-segment elevation in types 2 and 3 Brugada patterns. Two main hypotheses are debated for the underlying mechanisms of Brugada ECG patterns (7,9–13,23). The first is supported by canine RV wedge preparations that provided mechanistic support for a repolarization-related disorder (23). In brief, Brugada patterns appear to result from an abnormal transmural gradient of repolarization of the RV free wall and the RVOT, with heterogeneous reduction of the epicardial AP duration and
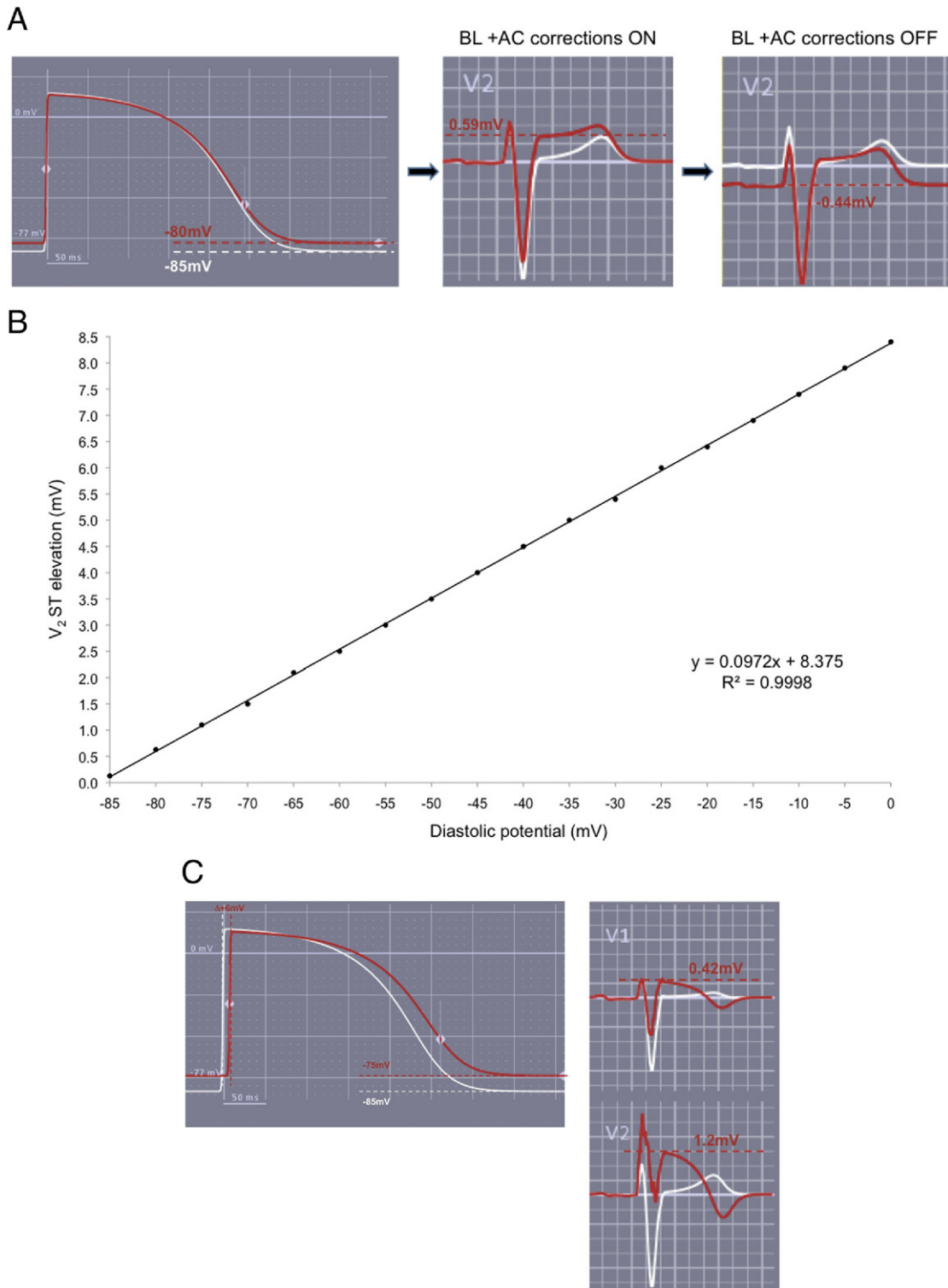
Figure 5 Simulation of Types 1 and 2 Brugada Patterns

(A) Representative example in which the diastolic potential of the center action potential (AP) was raised by 5 mV, which produced a 0.59-mV ST-segment elevation in lead V_2. Inactivation of the baseline (BL) and alternating-current (AC) corrections rendered the ST segment nearly isoelectric, while the TQ segment became depressed. **(B)** Linear relationship between the ST-segment elevation measured in lead V_2 and the diastolic potential of the selected region. **(C)** Attempt to simulate a type 1 Brugada ECG pattern in leads V_1 and V_2. Atypical right bundle branch block pattern with an ST-segment elevation and a negative T-wave were observed after introducing a small activation delay (center AP, +8 ms) and a moderate rise in the diastolic potential (center AP, +10 mV).

dome and unaltered endocardial APs causing ST-segment elevation with inverted T waves in the anterior chest leads. The second hypothesis states that the type 1 pattern results from delayed activation of the RVOT, leading to prolonged depolarization times and reversed repolarization forces, which inscribe negative T waves in the anterior chest leads (7,10,12). This hypothesis is indirectly supported by the recent observation that patients with BrS display fragmented potentials exclusively at the anterior aspect of the RVOT epicardium (10), by the presence of late potentials coinciding with delayed RVOT subepicardial activation (24,25) and by tissue Doppler studies showing delayed RV free wall contraction after AAD (26). Interestingly, none of the suspected alterations (AP shortening or activation delay) applied to the epicardial aspect of the RV free wall and RVOT reproduced the ST-segment elevation seen in types 2 and 3 Brugada ECG patterns. The mechanisms underlying ST-segment elevation during acute ischemia were discovered >30 years ago (27–29). Ischemic ST-segment elevation (as recorded with condenser-coupled amplifiers) is due to diastolic (TQ) depression and ST-segment elevation. TQ depression results from a rise in the diastolic potential of ischemic cells, which generate a current flow toward the nonischemic tissue and away from the recording electrode. ST-segment elevation, in turn, is produced by ischemic APs of reduced amplitude and plateau, which generate a current flow from the normal tissue toward the ischemic region and recording electrode. In these experiments, recordings of ECG direct-current potentials were made possible because the electrodes measured voltage differences with respect to a relative zero-reference potential fixed within the thorax (28). In ECG recording machines, however, because the real zero-reference potential remains unknown, baseline and alternating-current corrections set the TQ segment at zero potential, preventing the analysis of any diastolic alterations. Hence, any increase in diastolic potential will appear as an ST-segment elevation, not as a TQ depression. Recently, nodelike cells in the subepicardium of the RVOT were proposed as an arrhythmogenic source for BrS and other idiopathic arrhythmias (9,12). Nodelike cells have slower conduction properties and higher diastolic potentials (9,12). Using ECGSIM, the ST-segment elevations of types 2 and 3 Brugada patterns were reproduced by gradually raising diastolic potentials of the selected region. Figure 5A shows a representative example in which the diastolic potential of the center of the selected region was elevated by 5 mV (from −85 to −80 mV), producing an ST-segment elevation (5.9 mm at the J point) (Fig. 5A, middle) similar to that seen in a type 2 ECG pattern. Interestingly, the suppression of baseline and alternating-current corrections uncovered the underlying TQ depression (−0.44 mV) (Fig. 5A, right). Figure 5B highlights the linear relationship between the amplitude of the ST-segment elevation in lead V_2 and the diastolic potential of the selected region increased in 5-mV steps. Figure 5C shows an attempt to simulate a type 1 Brugada ECG pattern. Atypical RBBB pattern with ST-

segment elevation and negative T waves in leads V_1 and V_2 were obtained by raising the diastolic potential (by 10 mV) and delaying the activation (by 8 ms) for the selected region. Although speculative, these findings suggest that BrS may also comprise alterations of cellular mechanisms involved in the maintenance of the diastolic potential.

Study limitations. First, because the predictive values of our measurements were determined in referred patients, it is uncertain whether they apply to an unselected larger population. Second, the sensitivity of ajmaline challenge to unmask BrS is limited, because about 10% of SCN5A mutation carriers display negative results (30). Third, in ECGSIM, epicardial APs do not display the typical spike and dome features observed in wedge preparations (23). We were therefore unable to simulate the effect of heterogeneous RVOT AP configurations with and without spike and dome on the occurrence of the ST-segment elevation. Some investigators, however, did not observe loss of epicardial AP dome during open-heart surgery in patients with BrS (31).

REFERENCES

1. Brugada P, Brugada J. Right bundle branch block, persistent ST segment elevation and sudden cardiac death: a distinct clinical and electrocardiographic syndrome. A multicenter report. J Am Coll Cardiol 1992;20:1391–6.
2. Antzelevitch C, Brugada P, Borggrefe M, et al. Brugada syndrome: report of the second consensus conference: endorsed by the Heart Rhythm Society and the European Heart Rhythm Association. Circulation 2005;111:659–70.
3. Brugada R, Brugada J, Antzelevitch C, et al. Sodium channel blockers identify risk for sudden death in patients with ST-segment elevation and right bundle branch block but structurally normal hearts. Circulation 2000;101:510–5.
4. Patel SS, Anees S, Ferrick KJ. Prevalence of a Brugada pattern electrocardiogram in an urban population in the United States. Pacing Clin Electrophysiol 2009;32:704–8.
5. Pecini R, Cedergreen P, Theilade S, Haunso S, Theilade J, Jensen GB. The prevalence and relevance of the Brugada-type electrocardiogram in the Danish general population: data from the Copenhagen City Heart Study. Europace 2010;12:982–6.
6. Kadish AH, Buxton AE, Kennedy HL, et al. ACC/AHA clinical competence statement on electrocardiography and ambulatory electrocardiography: a report of the ACC/AHA/ACP-ASIM Task Force on Clinical Competence (ACC/AHA Committee to Develop a Clinical Competence Statement on Electrocardiography and Ambulatory Electrocardiography). J Am Coll Cardiol 2001;38:2091–100.
7. Hoogendijk MG, Opthof T, Postema PG, Wilde AA, de Bakker JM, Coronel R. The Brugada ECG pattern: a marker of channelopathy, structural heart disease, or neither? Toward a unifying mechanism of the Brugada syndrome. Circ Arrhythm Electrophysiol 2010;3:283–90.
8. Antzelevitch C. Brugada syndrome. Pacing Clin Electrophysiol 2006; 29:1130–59.

9. Elizari MV, Levi R, Acunzo RS, et al. Abnormal expression of cardiac neural crest cells in heart development: a different hypothesis for the etiopathogenesis of Brugada syndrome. Heart Rhythm 2007;4:359–65.
10. Nademanee K, Veerakul G, Chandanamattha P, et al. Prevention of ventricular fibrillation episodes in Brugada syndrome by catheter ablation over the anterior right ventricular outflow tract epicardium. Circulation 2011;123:1270–9.
11. Antzelevitch C. The Brugada syndrome: ionic basis and arrhythmia mechanisms. J Cardiovasc Electrophysiol 2001;12:268–72.
12. Meregalli PG, Wilde AA, Tan HL. Pathophysiological mechanisms of Brugada syndrome: depolarization disorder, repolarization disorder, or more? Cardiovasc Res 2005;67:367–78.
13. Wilde AA, Postema PG, Di Diego JM, et al. The pathophysiological mechanism underlying Brugada syndrome: depolarization versus repolarization. J Mol Cell Cardiol 2010;49:543–53.
14. van Oosterom A, Oostendorp TF. ECGSIM: an interactive tool for studying the genesis of QRST waveforms. Heart 2004;90:165–8.
15. DeLong ER, DeLong DM, Clarke-Pearson DL. Comparing the areas under two or more correlated receiver operating characteristic curves: a nonparametric approach. Biometrics 1988;44:837–45.
16. Durrer D. Electrical aspects of human cardiac activity: a clinical-physiological approach to excitation and stimulation. Cardiovasc Res 1968;2:1–18.
17. Lerecouvreux M, Perrier E, Leduc PA, et al. Right bundle branch block: electrocardiographic and prognostic features [article in French]. Arch Mal Coeur Vaiss 2005;98:1232–8.
18. Nakazawa K, Sakurai T, Kishi R, et al. Discrimination of Brugada syndrome patients from individuals with the saddle-back type ST-segment elevation using a marker of the standard 12-lead electrocardiography. Circ J 2007;71:546–9.
19. Hermida JS, Denjoy I, Jarry G, Jandaud S, Bertrand C, Delonca J. Electrocardiographic predictors of Brugada type response during Na channel blockade challenge. Europace 2005;7:447–53.
20. Di Diego JM, Fish JM, Antzelevitch C. Brugada syndrome and ischemia-induced ST-segment elevation. Similarities and differences. J Electrocardiol 2005;38:14–7.
21. Ogano M, Iwasaki YK, Morita N, et al. Proarrhythmic ECG deterioration caused by myocardial ischemia of the conus branch artery in patients with a Brugada ECG pattern. Pacing Clin Electrophysiol 2011;34:e26–9.
22. Shoji M, Yamashita T, Uejima T, et al. Electrocardiography characteristics of isolated non-compaction of ventricular myocardium in Japanese adult patients. Circ J 2010;74:1431–5.
23. Yan GX, Antzelevitch C. Cellular basis for the Brugada syndrome and other mechanisms of arrhythmogenesis associated with ST-segment elevation. Circulation 1999;100:1660–6.
24. Nagase S, Kusano KF, Morita H, et al. Epicardial electrogram of the right ventricular outflow tract in patients with the Brugada syndrome: using the epicardial lead. J Am Coll Cardiol 2002;39:1992–5.
25. Nagase S, Kusano KF, Morita H, et al. Longer repolarization in the epicardium at the right ventricular outflow tract causes type 1 electrocardiogram in patients with Brugada syndrome. J Am Coll Cardiol 2008;51:1154–61.
26. Tukkie R, Sogaard P, Vleugels J, de Groot IK, Wilde AA, Tan HL. Delay in right ventricular activation contributes to Brugada syndrome. Circulation 2004;109:1272–7.
27. Prinzmetal M, Toyoshima H, Ekmekci A, Mizuno Y, Nagaya T. Myocardial ischemia. Nature of ischemic electrocardiographic patterns in the mammalian ventricles as determined by intracellular electrographic and metabolic changes. Am J Cardiol 1961;8:493–503.
28. Kleber AG, Janse MJ, van Capelle FJ, Durrer D. Mechanism and time course of S-T and T-Q segment changes during acute regional myocardial ischemia in the pig heart determined by extracellular and intracellular recordings. Circ Res 1978;42:603–13.
29. Kjekshus JK, Maroko PR, Sobel BE. Distribution of myocardial injury and its relation to epicardial ST-segment changes after coronary artery occlusion in the dog. Cardiovasc Res 1972;6:490–9.
30. Veltmann C, Wolpert C, Sacher F, et al. Response to intravenous ajmaline: a retrospective analysis of 677 ajmaline challenges. Europace 2009;11:1345–52.
31. Kurita T, Shimizu W, Inagaki M, et al. The electrophysiologic mechanism of ST-segment elevation in Brugada syndrome. J Am Coll Cardiol 2002;40:330–4.

Key Words: Brugada syndrome ■ ECG criteria ■ ECGSIM ■ incomplete right bundle branch block.